

Multimode-cavity picture of non-Markovian waveguide QED

Dario Cilluffo¹, Luca Ferialdi², G. Massimo Palma^{2,3}, Giuseppe Calajò⁴ and Francesco Ciccarello^{2,3}

¹*Institut für Theoretische Physik and IQST, Albert-Einstein-Allee 11, Universität Ulm, 89069 Ulm, Germany*

²*Università degli Studi di Palermo, Dipartimento di Fisica e Chimica – Emilio Segrè, via Archirafi 36, I-90123 Palermo, Italy*

³*NEST, Istituto Nanoscienze-CNR, Piazza S. Silvestro 12, 56127 Pisa, Italy*

⁴*Istituto Nazionale di Fisica Nucleare (INFN), Sezione di Padova, I-35131 Padova, Italy*

(Dated: March 13, 2024)

We introduce a picture to describe and interpret waveguide-QED problems in the non-Markovian regime of long photonic retardation times resulting in delayed coherent feedback. The framework is based on an intuitive spatial decomposition of the waveguide into blocks. Among these, the block directly coupled to the atoms embodies an effective lossy multimode cavity leaking into the rest of the waveguide, in turn embodying an effective white-noise bath. The dynamics can be approximated by retaining only a finite number of cavity modes that yet eventually grows with the time delay. This description captures the atomic as well as the field's dynamics, even with many excitations, in both emission and scattering processes. As an application, we show that the recently identified non-Markovian steady states can be understood by retaining very few or even only one cavity modes.

Most quantum optics phenomena investigated so far occur under Markovian conditions (lack of memory effects). One major reason behind this is that atom-photon interaction is usually weak, while light travels very fast. This allows to neglect photonic time delays (retardation times), which is a tremendous simplification of the dynamics underpinning standard tools such as the Lindblad master equation and the input-output formalism [1]. Recent years have yet seen a growing attention to the *non-Markovian* regime of non-negligible photonic time delays, especially in the emerging area of waveguide Quantum ElectroDynamics (QED) which generally investigates the coherent interaction between quantum emitters and the one-dimensional (1D) field of a waveguide [2–4]. Such non-Markovian regime can today be accessed in some waveguide-QED experiments, e.g. through superconducting qubits coupled to surface acoustic waves [5] or slow-light modes (near a band edge) [6] and even cold atoms coupled to fiber-ring resonators [7]. While complicating the dynamics considerably, time delays can be leveraged for a variety of unprecedented phenomena and applications, such as persistent quantum beats [8], stabilization of Rabi oscillations [9–11], peculiar inelastic two-photon scattering [12, 13], generation of photonic cluster states [14], excitation of dressed bound states in the continuum [15–17], enhanced Dicke superradiance [18–21], anomalous population trapping [22], stationary oscillations of giant atoms [23], enhanced energy-time entanglement [24], improved single-photon sources [25], genuinely non-Markovian steady states [26].

From a merely computational viewpoint, it is well-established that such class of non-Markovian dynamics can be efficiently tackled via numerical methods [27–38] (moreover diagrammatic approaches were developed [39, 40]). Notwithstanding, mostly due the daunting complication of *delayed* (coherent) feedback, the underlying physics remains generally involved and non-trivial

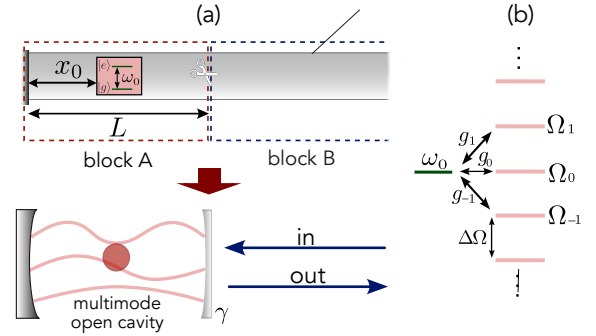


FIG. 1. Basic setup and idea. (a) A two-level atom is coupled to a semi-infinite waveguide, whose left end acts like a perfect mirror. We conveniently decompose the waveguide into a pair of blocks A and B mutually coupled with rate γ . Block A is an effective *multimode* and intrinsically *open* cavity (of length $L \gtrsim x_0$) in contact with block B (the latter one working as a semi-infinite waveguide itself). (b) Normal frequencies $\{\Omega_\nu\}$ of block A. The atom (energy ω_0) resonates with mode of frequency Ω_0 and is detuned from off-resonant modes $\Omega_{\pm 1}, \Omega_{\pm 2}, \dots$. The frequency spacing of A modes $\Delta\Omega$ scales as $\sim 1/\tau$ with $\tau = v/x_0$ the time delay, hence the stronger the non-Markovian effects, the larger is the number of A modes to account for. Notice that each frequency Ω_ν has width $\gamma \sim 1/\tau$ comparable with $\Delta\Omega$, reflecting the open nature of block A.

to interpret. In particular, to our knowledge, no simple picture to understand such dynamics was so far identified even in the weakly non-Markovian limit (i.e. the lowest non-trivial order in the characteristic time delay of the problem) where one could expect a relatively simple effective model capturing the essential physics to exist.

With the above motivations, this work introduces a physical picture for describing and interpreting non-Markovian waveguide-QED problems that is built upon a real-space decomposition of the waveguide into blocks. The essential idea is inspired by cavity QED, where non-negligible time delays occur if the atom couples signifi-

cantly to *many* cavity modes (see e.g. Refs. [41–43]): the longer the delay (say the time taken by a photon to reach a cavity mirror), the more cavity modes need to be considered. Of course, there is no actual cavity in a waveguide. Yet, nothing prevents one from viewing the latter as a set of communicating blocks [see blocks *A* and *B* in Fig. 1(a)] and treating the *finite*-size block directly coupled to the atom [i.e. block *A* in Fig. 1(a)] as an open cavity that leaks into the rest of the waveguide (this in turn described as a white-noise bath). If the size of the fictitious cavity [block *A* in Fig. 1(a)] is chosen to be comparable with the characteristic length of the problem, then the frequency spacing between block-*A* normal modes scales as the inverse of the characteristic time delay τ . Despite the relative arbitrariness of the block-*A* boundaries, it turns out that this picture allows to define an effective Hamiltonian that fully captures both (driven) emission and photon scattering, including many-excitation dynamics where atomic non-linearities are important.

System and basic parameters.—To present our theory, we will consider the case study where a two-level quantum emitter (henceforth called “atom”) is coupled to a semi-infinite waveguide [see Fig. 1(a)]. In spite of its apparent simplicity, this system hosts rich physics and is complex enough to show most salient effects of waveguide QED in the regime of long time delays (see e.g. Refs. [11, 14, 15, 26, 27, 36, 44–48]), which includes (via a suitable mapping) emission of a giant atom [5, 49] and even some paradigmatic sub- and super-radiance phenomena [18, 50]. The left end of the waveguide [see Fig. 1(a)] works as a perfect mirror placed at distance x_0 from the atom. The waveguide sustains a 1D field with linear dispersion $\omega = vk$ (with v the photon group velocity and k the wave vector). The atom’s ground and excited states $|g\rangle$ and $|e\rangle$, respectively, are separated in frequency by $\omega_0 = vk_0$; hence k_0 is the wave vector (modulus) of a photon resonant with the atom. Under weak

coupling (enabling the rotating-wave approximation), the Hamiltonian reads ($\hbar = 1$) [2–4]

$$H = \omega_0 \hat{\sigma}_+ \hat{\sigma}_- - iv \int_0^\infty dx \left[\hat{a}_R^\dagger(x) \partial_x \hat{a}_R(x) - \hat{a}_L^\dagger(x) \partial_x \hat{a}_L(x) \right] + g \int_0^\infty dx \left[\hat{\sigma}_+ (\hat{a}_L(x) + \hat{a}_R(x)) + \text{H.c.} \right] \delta(x - x_0), \quad (1)$$

with $\partial_x = \frac{d}{dx}$, $\hat{\sigma}_- = \hat{\sigma}_+^\dagger = |g\rangle\langle e|$, $\hat{a}_{R(L)}(x)$ the bosonic field operator annihilating a right-going (left-going) photon at position x and g the atom-photon coupling strength. This model is not analytically solvable in general, except for single-excitation dynamics (such as spontaneous emission or single-photon scattering [51]). The essential physical parameters are:

$$\Gamma = \frac{2g^2}{v}, \quad \tau = \frac{2x_0}{v}, \quad \phi = 2k_0 x_0. \quad (2)$$

Here, Γ is the standard decay rate that the atom would have without the feedback effect of the mirror (i.e. as if the waveguide were infinite, instead of ending at $x = 0$). Importantly, τ (*time delay*) is the time taken by a photon resonant with the atom to travel (twice) the atom-mirror distance and ϕ the corresponding accumulated phase. The strength of non-Markovian effects is measured by $\Gamma\tau$, quantifying how long is the time delay τ compared to the lifetime $1/\Gamma$. Thus, the Markovian regime occurs for $\Gamma\tau \ll 1$, while for growing $\Gamma\tau$ non-Markovian effects get stronger and stronger.

Effective model.—We view the waveguide as two joint “blocks” [see Fig. 1(a)]: block *A* (for $x \in [0, L[$ with $L > x_0$) and block *B* (for $x \geq L$). Importantly, *A* is the block directly coupled to the atom and has *finite* length. In contrast, block *B* (uncoupled from the atom) has infinite length and can be seen itself as a semi-infinite waveguide, yet having its left edge at $x = L$ [see Fig. 1(a)]. Based on such block-decomposition of the waveguide, by calling $\hat{\alpha}_\nu$ and $\hat{\beta}_\omega$ respectively the normal-mode (bosonic) ladder operators of blocks *A* and *B*, one can replace (1) with the effective Hamiltonian [52]

$$H_{\text{eff}} = \omega_0 \hat{\sigma}_+ \hat{\sigma}_- + \sum_\nu \Omega_\nu \hat{\alpha}_\nu^\dagger \hat{\alpha}_\nu + \int d\omega \omega \hat{\beta}_\omega^\dagger \hat{\beta}_\omega + \sqrt{\frac{\gamma}{2\pi}} \sum_\nu \int d\omega (\hat{\alpha}_\nu^\dagger \hat{\beta}_\omega + \text{H.c.}) + \sum_\nu g_\nu (\hat{\alpha}_\nu^\dagger \hat{\sigma}_- + \text{H.c.}), \quad (3)$$

where

$$\Omega_\nu = \omega_0 + v \frac{\nu\pi}{L}, \quad \gamma = \frac{2v}{L}, \quad (4)$$

$$g_\nu = g(-1)^\nu \sqrt{\frac{2}{L}} \sin\left(\frac{\nu\pi}{L} x_0 + \frac{\phi}{2}\right) \quad (5)$$

with ν running over all integers, while ω takes values throughout the real axis. The second (third) term of

Hamiltonian (3) describes the free Hamiltonian of block *A* (block *B*), where in particular Ω_ν [cf. Eq. (4)] are the normal frequencies of block *A* [see Fig. 1(b)]. The fourth term of (3) couples block *A* and block *B* with a characteristic rate γ given in Eq. (4) [notice that $1/\gamma$ is the characteristic time taken by a photon to leak out of block *A*]. Finally, the last term describes the coupling between the

atom and each block- A normal mode with corresponding coupling strength g_ν [see Fig. 1(b)]. The expression (5) of g_ν reflects the sinusoidal spatial shape of the A 's normal modes (just like a standard cavity-QED system). As a hallmark of the present framework, L (length of block A) is a free parameter of the model except for two conditions: (i) it must be strictly greater than x_0 to ensure that block A contains the atom, but in practice is required to be still comparable with x_0 (more on this later on); (ii) L must be a multiple integer of $\lambda_0/2$ with $\lambda_0 = 2\pi/k_0$ the atomic wavelength. Condition (ii) makes sure that there is a block- A mode resonant with the atom: this mode (henceforth called “resonant mode”) is labeled by $\nu = 0$ [indeed Eq. (4) yields $\Omega_{\nu=0} = \omega_0$].

Hamiltonian H_{eff} formally describes an effective cavity-QED system in that the atom is coupled to a multimode lossy cavity (block A) leaking into a white-noise photonic bath (embodied by block B). Notice that block A is an intrinsically *low-finesse* cavity: indeed [cf. Eqs. (4)] $\Delta\Omega = \Omega_{\nu+1} - \Omega_\nu \sim \gamma$, i.e. the frequency spacing $\Delta\Omega$ between A modes [cf. Fig. 1(b)] is comparable with the loss rate γ of block A . Physically, this stems from the inherently open nature of the fictitious cavity A which fully lacks the mirror at $x = L$.

To end up with (3), we resort to the standard discretization of a waveguide combined with weak coupling (the latter one allowing to linearize the dispersion law) [52]. Discretizing the system this way enables a clean definition of the two blocks, leading to a natural identification of their associated Hamiltonian and normal modes, whose continuous limit is eventually worked out.

Dependence on time delay.— The essence of the present picture is that the dynamics of the joint system can be effectively described by replacing Hamiltonian (1) with (3), where the latter can be approximated by retaining only a finite number of A modes which yet eventually grows with the time delay τ . To see the last key property, recall that we require L to be of the order of x_0 (e.g. $L = 2x_0$). Thus the spacing of A modes $\Delta\Omega = \pi\nu/L$ is of the order of τ^{-1} [see Eqs. (2), (4) and Fig. 1(b)], i.e. the detuning from the atom of the A modes with $|\nu| \geq 1$, henceforth called “off-resonant modes”, scales as the inverse of time delay (recall that block A is defined so as to ensure $\omega_0 = \Omega_0$). Accordingly, in the Markovian regime of vanishing τ all these off-resonant modes $|\nu| \geq 1$ are far-detuned from the atom so that only the resonant mode $\nu = 0$ needs to be accounted for [cf. Fig. 1(b)]. As the time delay grows up so that non-Markovian effects get increasingly important, more and more off-resonant modes must be retained in general. In other words, for given τ , one needs to retain all the modes $\nu = 0, \pm 1, \dots, \pm N_A$ with N_A eventually growing with τ . Thus the *multimode* nature of block A (instead of a more canonical one-mode cavity) reflects occurrence of retardation effects: while this is a well-known fact in standard cavity QED [41–43], the present framework pro-

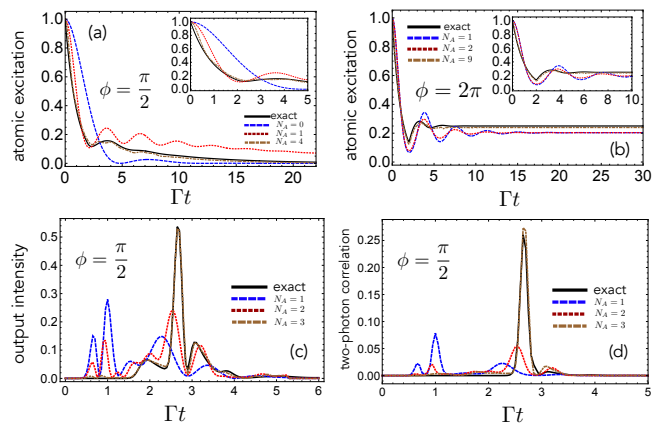


FIG. 2. (a) and (b): Atomic excitation, i.e. $\langle e|\rho|e\rangle = \rho_{ee}$ with ρ the atom’s density matrix, when the atom is initially in state $|e\rangle$ and the field in the vacuum state: exact analytical solution [44, 45] (black line) versus the approximated using Eq. (3) by retaining only modes $\nu = 0, \pm 1, \dots, \pm N_A$ for $\phi = \pi/2$ (a) and $\phi = 2\pi$ (b). We set $\Gamma\tau = 2$. (c)-(d) Field’s output intensity (c) and two-photon correlation function (d) after the scattering of a left-incoming Gaussian coherent wave packet (see [52]). We set the wave packet’s width to $W = 2.5\Gamma$ and the average number of photons to $n_{\text{ph}} = 0.5$ with phase $\phi = \pi/2$ and delay $\Gamma\tau = 4$. In (a)-(d), we set $L = 2x_0$.

vides ground to take advantage of this property also in the study of *waveguide*-QED systems.

Testing the framework.—To check the effectiveness of the waveguide decomposition into blocks, in Fig. 2 we set $L = 2x_0$, $\Gamma\tau \geq 2$ (relatively long delay) and the representative phase $\phi = \pi/2$ [except for panel (b) where $\phi = 2\pi$] for two paradigmatic dynamics: spontaneous emission [panels (a)-(b)] and scattering of a coherent-state wave packet [(c)-(d)].

In each case, the dynamics predicted by the effective model in Eq. (3) by retaining only the A modes $\nu = 0, \pm 1, \dots, \pm N_A$ is compared with the exact solution of (1) obtained through either analytical methods when available [as in the single-excitation dynamics of panels (a)-(b)] or numerical simulations based on Matrix Product States [27] [panels (c)-(d)]. As N_A is made larger, the mismatch between exact and approximated dynamics gets smaller and smaller until becoming negligible, including the special value of phase $\phi = 2\pi$ in Fig. 2(b) where it is known that the atom does not fully decay [44, 45]. Notice that, unlike Figs. 2(a) and (b), the dynamics in panels (c)-(d) involves many excitations, providing evidence that the picture is effective even when the atom’s intrinsic nonlinearity has substantial effects. This is especially striking in panel Fig. 2(d), reporting the two-photon correlation function of scattered light, which clearly shows a multi-photon peak [this adds to the delayed single-photon peak of the output intensity in panel (c)]. Analogous conclusions hold for different settings of the parameters.

We note that the convergence rate is generally affected by ϕ and L , a major reason being the sinusoidal dependence on these parameters of the coupling strength g_ν [cf. Eq. (5)]. For analogous reasons, in general the convergence is not strictly monotonic, i.e. it can happen that $N_A + 1$ modes perform as N_A or even worse [52]. Notwithstanding, convergence eventually occurs because $|g_\nu| \leq g\sqrt{2/L}$ for any ν while the detuning $|\Omega_\nu - \omega_0|$ grows linearly with ν [cf. Eqs. (4)-(5)]. Although somewhat implicit in the above, it is worth stressing here that the advantage of the framework is not to provide a fast computational numerical tool (where efficient techniques exist already) but rather an intuitive physical picture connecting non-Markovian waveguide QED with cavity QED. This is illustrated next with some important instances.

Markovian limit and Purcell effect.— For $\Gamma\tau \ll 1$ we are in the Markovian regime: time delay is negligible, but the feedback provided by the mirror affects atomic emission resulting in a decay rate modulated by ϕ as $\Gamma'(\phi) = 2\Gamma \sin^2 \frac{\phi}{2}$ [44, 45], which was experimentally confirmed [53]. Thus emission can be either enhanced or suppressed; in particular $\Gamma' = 2\Gamma$ for $\phi = (2m + 1)\pi$ while $\Gamma' = 0$ for $\phi = 2m\pi$ (m is an integer). Now, using our framework, we see that, due to $\Delta\Omega \sim 1/\tau$ [cf. Eq. (5)], for negligible τ the off-resonant modes of block A are very far-detuned from the atom and thus can be neglected. Only the resonant mode $\nu = 0$ thus needs to be accounted for. Its bandwidth is yet very large since we also have $\gamma \sim \Delta\Omega \sim 1/\tau$ [cf. Eq. (5)]. The system therefore reduces to an atom coupled to a standard one-mode cavity, but in the *bad cavity* limit. The corresponding atom-mode coupling strength is $g_0 = g\sqrt{\frac{2}{L}} \sin \frac{\phi}{2}$ [cf. Eq. (5)], which indeed vanishes for $\phi = 2m\pi$ meaning that in this case the atom sits right on a cavity field's node and is thus unable to emit. Standard cavity-QED theory (bad-cavity limit) then predicts the decay rate $4g_0^2/\gamma$, which indeed exactly matches $\Gamma'(\phi)$. This shows that the action of the mirror, despite no actual cavity is present, can still be seen as a manifestation of the standard Purcell effect in a cavity.

Non-Markovian steady states.—Recently, Ask and Johansson showed that a driven atom in front of a mirror for non-negligible $\Gamma\tau$ can reach steady states unattainable in a standard Markovian bath [26]. Specifically, let

$$\dot{\hat{\rho}} = -i \left[\frac{1}{2}\Omega_D \hat{\sigma}_x, \hat{\rho} \right] \kappa \mathcal{D}[\hat{\sigma}_-] \hat{\rho} + \kappa_\phi \mathcal{D}[\hat{\sigma}_+ \hat{\sigma}_-] \quad (6)$$

with $\mathcal{D}[A]\hat{\rho} = A\hat{\rho}A^\dagger - \frac{1}{2}\{A^\dagger A, \hat{\rho}\}$, be the standard Markovian master equation (ME) of an atom subject to a classical drive of Rabi frequency Ω_D , pure dephasing with rate κ_ϕ and decaying into a Markovian bath with rate κ . An atom's state ρ is fully specified by the (excited-state) population ρ_{ee} and coherence ρ_{eg} . After a transient, the emitter reaches a steady state obtained by imposing $\dot{\hat{\rho}} = 0$ in Eq. (6). It turns out that, irrespective of

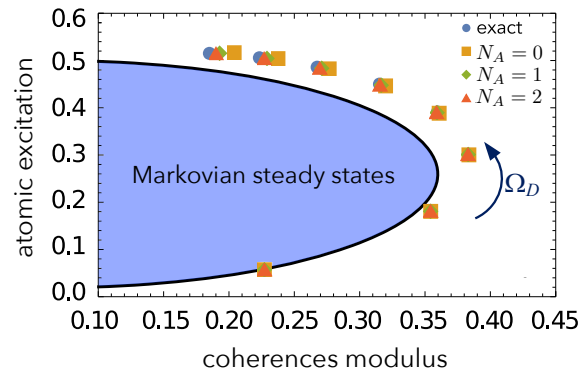


FIG. 3. Non-Markovian steady states. Each point of the plane has coordinates $(|\rho_{eg}|, \rho_{ee})$, with ρ_{eg} (ρ_{ee}) the coherences (excited-state population) of a possible steady state $\hat{\rho}$ of a driven atom emitting into the semi-infinite waveguide. Emission into a Markovian bath [see Eq. (6)] can only yield steady states within the shaded area [54]. The blue dots are exact steady states computed through MPS simulations for Rabi frequencies (in units of Γ) $\Omega_D = 0.5, 1, 1.5, 2, 2.5, 3, 3.5, 4$ from bottom to top (as shown by the curved arrow) and for $\Gamma\tau = 0.25$ and $\phi = \pi$. The other points (squares, rhombi and triangles) are approximated steady states calculated through the effective Hamiltonian (3) by retaining N_A modes of block A for $L = x_0$.

Ω and κ , the steady state must lie within the shaded region bounded by the elliptical line shown in Fig. 3. This bound in particular holds for a driven atom in a semi-infinite waveguide in the Markovian regime $\Gamma\tau \ll 1$ (see previous section). Yet, it can be violated in the non-Markovian regime: see e.g. the blue dots in Fig. 3 computed via exact MPS numerical simulations [26, 52] corresponding to the steady states occurring for $\Gamma\tau = 0.25$, $\phi = \pi$ and (from bottom to top, see curved arrow) growing values of Ω_D .

The steady states in Fig. 3 can be well-approximated using our block-decomposition framework, as shown by Fig. 3 where the agreement with the exact solution (blue dots) grows with N_A . Remarkably, retaining even a *single* cavity mode ($N_A = 0$; orange squares) provides an excellent quantitative approximation at low values of Ω_L/Γ and, as long as population ρ_{ee} is concerned, even at larger ones; in any case, on a qualitative ground, it appears to capture most of the relevant physics. In this case, the emitter's steady state can be obtained through partial trace from the bipartite Markovian ME governing the evolution of $\hat{\rho}$ (joint state of the atom and mode $\nu = 0$)

$$\dot{\hat{\rho}} = -i \left[\frac{1}{2}\Omega_D \hat{\sigma}_x + g_0(\hat{\alpha}_0^\dagger \hat{\sigma}_- + \text{H.c.}), \hat{\rho} \right] + \gamma \mathcal{D}[\hat{\alpha}_0] \hat{\rho}, \quad (7)$$

with γ and g_0 given by Eqs. (4) and (5). We point out that occurrence of population inversion at long times, i.e. $\rho_{ee} > 1/2$, is a sufficient condition to reach non-Markovian steady states beyond the elliptical bound in Fig. 3. Occurrence of population inversion for a driven two-level system coupled to a lossy cavity mode is a well-

established quantum optics effect [55], which highlights a further interesting connection between non-Markovian waveguide QED and cavity QED.

Conclusions.— We presented a picture to describe and interpret waveguide-QED dynamics with delayed feedback. After decomposing the waveguide into blocks, the block coupled to the atom is viewed as an open cavity leaking into the rest of the waveguide. The longer the time delay, the more modes of such open cavity generally need to be accounted for. The picture captures both the atom and field dynamics, even when many excitations are present.

The idea that atoms in waveguides could be understood in terms of effective cavities appeared several times (see e.g. Refs. [54, 56–58]), sometimes relying on the well-known mirror-like behaviour of an atom [59]. In contrast, the cavity central to our framework relies on a fully transparent fictitious mirror. Yet, it is instrumental to the establishment of a sharp link between emission phenomena featuring delayed feedback and cavity-QED physics with the bonus that the picture can capture the waveguide-field dynamics as well. Our theory can be seen to define a (so called) Markovian embedding (or dilation) in the following sense: one replaces an open system (the atom in our case) immersed in a non-Markovian bath with an enlarged open system (atom plus A modes here) that is instead immersed in a Markovian bath. This is arguably the most common strategy to attack non-Markovian problems and is typically accomplished by adding auxiliary lossy modes to the open system [36, 60–63]. Two remarkable features yet stand out in the present approach: (i) the open-cavity modes have a clear physical meaning and can be straightforwardly visualized as degrees of freedom taken out of the bath (i.e. the waveguide); (ii) besides the open system, the framework can describe as well the bath dynamics. We anticipate that this work could offer a novel alternative approach to understanding and interpreting waveguide-QED phenomena within the relatively unexplored non-Markovian regime.

D.C. acknowledges support from the BMBF project PhoQuant (grant no. 13N16110) and the state of Baden-Württemberg through bwHPC and the German Research Foundation (DFG) through grant no. INST 40/575-1 FUGG (JUSTUS 2 cluster). G.M.P. acknowledges support from MUR under PRIN Project no. 2022FEXLYB “Quantum Reservoir Computing” (QuReCo). G.C. acknowledges that results incorporated in this standard have received funding from the T-NiSQ consortium agreement financed by QUANTERA 2021. Numerical simulations were performed using QuTip [64] and mpnum [65]. F.C. acknowledges support from European Union – Next Generation EU through Project Eurostart 2022 “Topological atom-photon interactions for quantum tech-

nologies” (MUR D.M. 737/2021) and through Project PRIN 2022-PNRR no. P202253RLY “Harnessing topological phases for quantum technologies”.

-
- [1] C. Gardiner and P. Zoller, *Quantum Noise: A Handbook of Markovian and Non-Markovian Quantum Stochastic Methods with Applications to Quantum Optics*, 3rd ed., Springer Series in Synergetics (Springer-Verlag, Berlin Heidelberg, 2004).
 - [2] Z. Liao, X. Zeng, H. Nha, and M. S. Zubairy, *Physica Scripta* **91**, 63004 (2016).
 - [3] D. Roy, C. M. Wilson, and O. Firstenberg, *Reviews of Modern Physics* **89**, 21001 (2017).
 - [4] A. S. Sheremet, M. I. Petrov, I. V. Iorsh, A. V. Poshakinskiy, and A. N. Poddubny, *Rev. Mod. Phys.* **95**, 015002 (2023).
 - [5] G. Andersson, B. Suri, L. Guo, T. Aref, and P. Delsing, *Nature Physics* **15**, 1123–1127 (2019).
 - [6] V. S. Ferreira, J. Banker, A. Sipahigil, M. H. Matheny, A. J. Keller, E. Kim, M. Mirhosseini, and O. Painter, *Phys. Rev. X* **11**, 041043 (2021).
 - [7] D. Lechner, R. Pennetta, M. Blaha, P. Schneeweiss, A. Rauschenbeutel, and J. Volz, *Phys. Rev. Lett.* **131**, 103603 (2023).
 - [8] H. Zheng and H. U. Baranger, *Physical Review Letters* **110**, 113601 (2013).
 - [9] A. Carmele, J. Kabuss, F. Schulze, S. Reitzenstein, and A. Knorr, *Physical Review Letters* **110**, 13601 (2013).
 - [10] J. Kabuss, D. O. Krimer, S. Rotter, K. Stannigel, A. Knorr, and A. Carmele, *Phys. Rev. A* **92**, 053801 (2015).
 - [11] A. L. Grimsmo, *Physical Review Letters* **115**, 60402 (2015).
 - [12] M. Laakso and M. Pletyukhov, *Physical Review Letters* **113**, 183601 (2014).
 - [13] Y. L. L. Fang and H. U. Baranger, *Physical Review A* **91**, 53845 (2015), arXiv:1502.03803.
 - [14] H. Pichler, S. Choi, P. Zoller, and M. D. Lukin, *Proceedings of the National Academy of Sciences* **114**, 11362 (2017).
 - [15] G. Calajó, Y.-L. L. Fang, H. U. Baranger, and F. Ciccarello, *Physical Review Letters* **122**, 073601 (2019).
 - [16] R. Trivedi, D. Malz, S. Sun, S. Fan, and J. Vučković, *Phys. Rev. A* **104**, 013705 (2021).
 - [17] K. Barkemeyer, A. Knorr, and A. Carmele, *Phys. Rev. A* **103**, 033704 (2021).
 - [18] K. Sinha, P. Meystre, E. A. Goldschmidt, F. K. Fatemi, S. L. Rolston, and P. Solano, *Phys. Rev. Lett.* **124**, 043603 (2020).
 - [19] F. Dinc and A. M. Brańczyk, *Phys. Rev. Res.* **1**, 032042 (2019).
 - [20] K. Sinha, A. González-Tudela, Y. Lu, and P. Solano, *Phys. Rev. A* **102**, 043718 (2020).
 - [21] C. A. González-Gutiérrez, J. Román-Roche, and D. Zueco, *Phys. Rev. A* **104**, 053701 (2021).
 - [22] A. Carmele, N. Nemet, V. Canela, and S. Parkins, *Phys. Rev. Res.* **2**, 013238 (2020).
 - [23] L. Guo, A. F. Kockum, F. Marquardt, and G. Johansson, *Phys. Rev. Research* **2**, 043014 (2020).
 - [24] K. Barkemeyer, M. Hohn, S. Reitzenstein, and

- A. Carmele, *Phys. Rev. A* **103**, 062423 (2021).
- [25] G. Crowder, L. Ramunno, and S. Hughes, “Improving on-demand single photon source coherence and indistinguishability through a time-delayed coherent feedback,” (2023), [arXiv:2302.08093 \[quant-ph\]](#).
- [26] A. Ask and G. Johansson, *Phys. Rev. Lett.* **128**, 083603 (2022).
- [27] H. Pichler and P. Zoller, *Physical Review Letters* **116**, 93601 (2016).
- [28] T. Ramos, B. Vermersch, P. Hauke, H. Pichler, and P. Zoller, *Phys. Rev. A* **93**, 062104 (2016).
- [29] R. Trivedi, K. Fischer, S. D. Mishra, and J. Vučković, *Phys. Rev. A* **100**, 043827 (2019).
- [30] S. J. Whalen, *Phys. Rev. A* **100**, 052113 (2019).
- [31] Y.-L. L. Fang, *Computer Physics Communications* **235**, 422 (2019).
- [32] F. Dinc, İ. Ercan, and A. M. Brańczyk, *Quantum* **3**, 213 (2019).
- [33] G. Crowder, H. Carmichael, and S. Hughes, *Phys. Rev. A* **101**, 023807 (2020).
- [34] S. Arranz Regidor, G. Crowder, H. Carmichael, and S. Hughes, *Phys. Rev. Res.* **3**, 023030 (2021).
- [35] G. Crowder, L. Ramunno, and S. Hughes, *Phys. Rev. A* **106**, 013714 (2022).
- [36] X. H. Zhang, S. Klapp, and A. Metelmann, arXiv preprint [arXiv:2204.02367](#) (2022).
- [37] K. Barkemeyer, A. Knorr, and A. Carmele, *Phys. Rev. A* **106**, 023708 (2022).
- [38] K. Vodenkova and H. Pichler, [arXiv:2311.07302](#).
- [39] F. Dinc, *Phys. Rev. A* **102**, 013727 (2020).
- [40] K. Piasotski and M. Pletyukhov, *Phys. Rev. A* **104**, 023709 (2021).
- [41] P. W. Milonni, J. R. Ackerhalt, H. W. Galbraith, and M.-L. Shih, *Phys. Rev. A* **28**, 32 (1983).
- [42] R. J. Cook and P. W. Milonni, *Physical Review A* **35**, 5081 (1987).
- [43] D. O. Krimer, M. Liertzer, S. Rotter, and H. E. Türeci, *Phys. Rev. A* **89**, 033820 (2014).
- [44] U. Dorner and P. Zoller, *Physical Review A* **66**, 1 (2002).
- [45] T. Tufarelli, F. Ciccarello, and M. S. Kim, *Physical Review A* **87**, 13820 (2013).
- [46] T. Tufarelli, M. S. Kim, and F. Ciccarello, *Physical Review A* **90**, 12113 (2014).
- [47] P. O. Guimond, M. Pletyukhov, H. Pichler, and P. Zoller, *Quantum Science and Technology* **2**, 44012 (2017), [arXiv:1706.07844](#).
- [48] E. Wiegand, B. Rousseaux, and G. Johansson, *Phys. Rev. A* **101**, 033801 (2020).
- [49] L. Guo, A. Grimsmo, A. F. Kockum, M. Pletyukhov, and G. Johansson, *Physical Review A* **95**, 53821 (2017), [arXiv:1612.00865](#).
- [50] C. Gonzalez-Ballester, E. Moreno, F. J. Garcia-Vidal, and A. Gonzalez-Tudela, *Physical Review A* **94**, 63817 (2016), [arXiv:1608.04928](#).
- [51] Y. L. L. Fang, F. Ciccarello, and H. U. Baranger, *New Journal of Physics* **20**, 43035 (2018).
- [52] See Supplemental Material at xxx for technical details.
- [53] I. C. Hoi, A. F. Kockum, L. Tornberg, A. Pourkabirian, G. Johansson, P. Delsing, and C. M. Wilson, *Nature Physics* **11**, 1045 (2015).
- [54] A. Ask, M. Ekström, P. Delsing, and G. Johansson, *Phys. Rev. A* **99**, 013840 (2019).
- [55] M. Lindberg and C. M. Savage, *Physical Review A* **38**, 5182 (1988).
- [56] D. E. Chang, L. Jiang, A. V. Gorshkov, and H. J. Kimble, *New Journal of Physics* **14**, 63003 (2012).
- [57] E. Wiegand, B. Rousseaux, and G. Johansson, *Phys. Rev. Res.* **3**, 023003 (2021).
- [58] S. Arranz Regidor and S. Hughes, *Phys. Rev. A* **108**, 033719 (2023).
- [59] J. T. Shen and S. Fan, *Optics Letters* **30**, 2001 (2005).
- [60] D. Tamascelli, A. Smirne, S. F. Huelga, and M. B. Plenio, *Phys. Rev. Lett.* **120**, 030402 (2018).
- [61] S. Campbell, F. Ciccarello, G. M. Palma, and B. Vacchini, *Phys. Rev. A* **98**, 012142 (2018).
- [62] R. Trivedi, D. Malz, and J. I. Cirac, *Phys. Rev. Lett.* **127**, 250404 (2021).
- [63] A. Nüßeler, D. Tamascelli, A. Smirne, J. Lim, S. F. Huelga, and M. B. Plenio, *Phys. Rev. Lett.* **129**, 140604 (2022).
- [64] J. Johansson, P. Nation, and F. Nori, *Computer Physics Communications* **183**, 1760 (2012).
- [65] D. Suess and M. Holzäpfel, *Journal of Open Source Software* **2**, 465 (2017).

Supplemental Material for “Multimode-cavity picture of non-Markovian waveguide QED”

D. Cilluffo,¹ L. Ferialdi,² G. M. Palma,^{2,3} G. Calajò,⁴ and F. Ciccarello^{2,3}

¹*Institut für Theoretische Physik and IQST, Albert-Einstein-Allee 11, Universität Ulm, 89069 Ulm, Germany*

²*Università degli Studi di Palermo, Dipartimento di Fisica e Chimica – Emilio Segrè, via Archirafi 36, I-90123 Palermo, Italy*

³*NEST, Istituto Nanoscienze-CNR, Piazza S. Silvestro 12, 56127 Pisa, Italy*

⁴*Istituto Nazionale di Fisica Nucleare (INFN), Sezione di Padova, I-35131 Padova, Italy*

(Dated: March 13, 2024)

DERIVATION OF THE EFFECTIVE HAMILTONIAN

Here we derive the effective Hamiltonian (3) by first discretizing the waveguide, then decomposing it into blocks and finally taking the continuous limit. We start with a review of the discretization of a continuous waveguide.

Discretized waveguide: review

Consider a homogeneous coupled-cavity array with cavities located at positions n , whose free Hamiltonian has the usual tight-binding form

$$\hat{H}_F = \omega_c \sum_n \hat{a}_n^\dagger \hat{a}_n - J \sum_n (\hat{a}_{n+1}^\dagger \hat{a}_n + \text{H.c.}), \quad (\text{S1})$$

with ω_c the frequency of each cavity and J the cavity-cavity hopping rate.

Under periodic boundary conditions ($\hat{a}_1 \equiv \hat{a}_{N+1}$) the waveguide’s normal modes are the usual plane waves with dispersion law

$$\omega_k = \omega_c - 2J \cos k, \quad (\text{S2})$$

which gives rise to an energy band of width $4J$, where $k_m = 2\pi m/(N+1)$ with $m = 1, \dots, N$. The corresponding group velocity is $v_k = d\omega/dk = 2J \sin k$, hence (far from the band edges) the dispersion law can be linearized around a specific wavevector k_0 as $\omega_k \simeq (\omega_c - 2J \cos k_0) + v(k - k_0)$ with $v = v_{k_0}$.

In the presence of an atom coupled to the waveguide at position n_0 , the total Hamiltonian reads

$$\hat{H} = \omega_0 \hat{\sigma}_+ \hat{\sigma}_- + \hat{H}_F + \hat{V}_{AF}. \quad (\text{S3})$$

with the atom-field interaction Hamiltonian given by

$$\hat{V}_{AF} = g (\hat{\sigma}_+ \hat{a}_{n_0} + \text{H.c.}). \quad (\text{S4})$$

Note that the coupling-strength g here is defined differently from the one in Eq. (1) of the main text, and indeed they have different dimensions. If the atom is tuned inside the photonic band (i.e. $\omega_c - 2J < \omega_0 < \omega_c + 2J$), only photonic modes of frequency ω_k close to ω_0 need to be considered, hence one can linearize the dispersion law around $\pm k_0$ with k_0 defined by $\omega_0 = \omega_{k_0}$. It can be shown that the real-space representation of the linearized field’s Hamiltonian so obtained is analogous to the second term of (1).

If we now consider *open* boundary conditions, such that $\hat{a}_0 = \hat{a}_{N+1} = 0$, the spectrum (S2) is unaffected but the normal modes now have sinusoidal shape

$$\hat{\alpha}_m = \sqrt{\frac{2}{N+1}} \sum_{n=1}^N \sin(k_m n) \hat{a}_n \quad \text{with} \quad k_m = \frac{\pi m}{N+1} \quad \text{for} \quad m = 1, \dots, N. \quad (\text{S5})$$

In the limit $N \rightarrow \infty$ we obtain a semi-infinite waveguide (or equivalently a waveguide subject to a hard-wall boundary condition at $n = 0$).

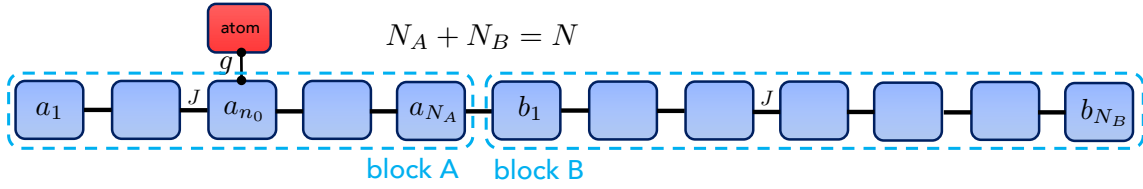


FIG. S1. Decomposition of the discretized waveguide into blocks A and B with $b_1 \equiv a_{N_A+1}, \dots, b_{N_B} \equiv a_N$. Note that $N_A \geq n_0$, meaning that block A is directly coupled to the atom.

Decomposition into blocks

We start from Hamiltonian (S1) under open boundary conditions and split the discretized waveguide in two blocks (see Fig. S1): block A for $1 \leq n \leq N_A$ with $N_A \geq n_0$ and block B for $N_A + 1 \leq n \leq N$ (so that block A is the one of the two directly coupled to the atom). Corresponding to this block decomposition, we rearrange the free field's Hamiltonian as

$$\hat{H}_F = \underbrace{\omega_c \sum_{n=1}^{N_A} \hat{a}_n^\dagger \hat{a}_n - J \sum_{n=1}^{N_A-1} (\hat{a}_n \hat{a}_{n+1}^\dagger + \text{H.c.})}_{\hat{H}_A} + \underbrace{\omega_c \sum_{n=1}^{N_B} \hat{b}_n^\dagger \hat{b}_n - J \sum_{n=1}^{N_B-1} (\hat{b}_n \hat{b}_{n+1}^\dagger + \text{H.c.})}_{\hat{H}_B} - \underbrace{J (\hat{a}_{N_A} \hat{b}_1^\dagger + \text{H.c.})}_{\hat{V}_{AB}} \quad (\text{S6})$$

where $N_B = N - N_A$ is the size of block B . Notice that for convenience we have re-named the bosonic site modes of block B as $\hat{b}_n = \hat{a}_{n-N_A}$. In Eq. (S6), \hat{H}_A (\hat{H}_B) is the free Hamiltonian of block A (block B). It is important to stress that the two blocks are mutually *coupled* with interaction Hamiltonian \hat{V}_{AB} and coupling strength just equal to the photon hopping rate J : their coupling guarantees a photon coming from block A to reach B (or the other way around) without suffering any back-reflection.

The sine-shaped normal modes of block A read [compare with Eq. (S5)]

$$\hat{\alpha}_m = \sqrt{\frac{2}{N_A + 1}} \sum_{n=1}^{N_A} \sin(k_m^A n) \hat{a}_n \quad \text{with} \quad k_m^A = \frac{\pi m}{N_A + 1} \quad \text{for} \quad m = 1, \dots, N_A. \quad (\text{S7})$$

In terms of these, the free Hamiltonian of block A takes the diagonal form

$$\hat{H}_A = \sum_{m=1}^{N_A} \omega_m^A \hat{\alpha}_m^\dagger \hat{\alpha}_m, \quad (\text{S8})$$

where $\omega_m^A = \omega_c - 2J \cos k_m^A$. Real-space block- A operators can be expressed in terms of these normal modes as

$$\hat{a}_n = \sqrt{\frac{2}{N_A + 1}} \sum_{m=1}^{N_A} \sin(k_m^A n) \hat{\alpha}_m. \quad (\text{S9})$$

This allows us to express even the atom-field interaction Hamiltonian (S4) in terms of the A 's normal modes as

$$\hat{V}_{AF} = \sum_{m=1}^{N_A} g_m (\hat{\sigma}_+ \hat{\alpha}_m + \text{H.c.}), \quad (\text{S10})$$

where g_m measures how strongly is the atom coupled to the m -th normal mode of block A

$$g_m = g \sqrt{\frac{2}{N_A + 1}} \sin(k_m^A n_0). \quad (\text{S11})$$

Likewise, using the same decomposition (S9) for $n = N_A$, the coupling Hamiltonian between blocks A and B [cf. Eq. (S6)] is arranged as

$$\hat{V}_{AB} = -J \sqrt{\frac{2}{N_A + 1}} \sum_{m=1}^{N_A} \sin(k_m^A N_A) \hat{\alpha}_m \hat{b}_1^\dagger = \sum_{m=1}^{N_A} \xi_m (\hat{\alpha}_m \hat{b}_1^\dagger + \text{H.c.}), \quad (\text{S12})$$

where we defined

$$\xi_m = J \sqrt{\frac{2}{N_A + 1}} (-1)^m \sin\left(\frac{m\pi}{N_A + 1}\right), \quad (\text{S13})$$

and used the identity

$$\sin(k_m^A N_A) = -(-1)^m \sin(k_m^A). \quad (\text{S14})$$

Analogously to block A , we can define normal modes also for block B as [cf. Eq. (S9)]

$$\hat{\beta}_m = \sqrt{\frac{2}{N_B + 1}} \sum_{n=1}^{N_B} \sin(k_m^B n) \hat{b}_n \quad \text{with} \quad k_m^B = \frac{\pi m}{N_B + 1} \quad \text{for} \quad m = 1, \dots, N_B \quad (\text{S15})$$

such that [cf. Eq. (S8)] $\hat{H}_B = \sum_{m=1}^{N_A} \omega_m^B \hat{\beta}_m^\dagger \hat{\beta}_m$ with $\omega_m^B = \omega_c - 2J \cos k_m^B$. The inverse transformation reads

$$\hat{b}_n = \sqrt{\frac{2}{N_B + 1}} \sum_{m=1}^{N_B} \sin(k_m^B n) \hat{\beta}_m, \quad (\text{S16})$$

and allows now to arrange the A - B interaction Hamiltonian (S12) as

$$\hat{V}_{AB} = \sum_{m=1}^{N_A} \sum_{m'=1}^{N_B} \xi_m \chi_{m'} \left(\hat{\alpha}_m \hat{\beta}_{m'}^\dagger + \text{H.c.} \right). \quad (\text{S17})$$

with

$$\chi_m = \sqrt{\frac{2}{N_B + 1}} \sin\left(\frac{m\pi}{N_B + 1}\right) \quad (\text{S18})$$

To summarize, in terms of block- A and block- B normal modes the total Hamiltonian reads

$$\hat{H} = \omega_0 \hat{\sigma}_+ \hat{\sigma}_- + \underbrace{\sum_{m=1}^{N_A} \omega_m^A \hat{\alpha}_m^\dagger \hat{\alpha}_m + \sum_{m=1}^{N_B} \omega_m^B \hat{\beta}_m^\dagger \hat{\beta}_m + \sum_{m=1}^{N_A} \sum_{m'=1}^{N_B} \xi_m \chi_{m'} \left(\hat{\alpha}_m \hat{\beta}_{m'}^\dagger + \text{H.c.} \right)}_{=\hat{H}_F} + \underbrace{\sum_{m=1}^{N_A} g_m (\hat{\sigma}_+ \hat{\alpha}_m + \text{H.c.})}_{=\hat{V}_{AF}} \quad (\text{S19})$$

where we recall that

$$\omega_m^A = \omega_c - 2J \cos k_m^A, \quad \omega_m^B = \omega_c - 2J \cos k_m^B. \quad (\text{S20})$$

Continuous limit and linearization

Since we are considering a semi-infinite waveguide, the length of block B must diverge as $N_B \rightarrow \infty$. Accordingly, block- B normal ladder operators $\{\hat{\beta}_m\}$ become a continuum of singular bosonic modes $\{\hat{\beta}(k)\}$ with $0 \leq k < \pi$ fulfilling $[\hat{\beta}(k), \hat{\beta}^\dagger(k')] = \delta(k - k')$. Specifically, $\hat{\beta}(k)$ is obtained as the continuous limit of the rescaled ladder operators $\hat{\beta}_m / \sqrt{\Delta k}$ with $\Delta k = 2\pi/N_B$. This way, in Hamiltonian (S19) we can make the replacements

$$\sum_{m=1}^{N_B} \omega_m^B \hat{\beta}_m^\dagger \hat{\beta}_m \rightarrow \int_0^\pi dk \omega^B(k) \hat{\beta}^\dagger(k) \hat{\beta}(k), \quad \sum_{m'=1}^{N_B} \chi_{m'} \hat{\beta}_{m'} \rightarrow \int_0^\pi dk \sqrt{\frac{2}{\pi}} \sin k \hat{\beta}(k). \quad (\text{S21})$$

Here, in each sum we multiplied and divided the summand by Δk , expressed it in terms of $\hat{\beta}_m / \sqrt{\Delta k}$ and finally carried out the continuous limit thus turning sums into integrals over the first Brillouin zone.

We assume now that the atom is tuned on resonance with a specific normal mode of block A whose wavevector labeled by $m = m_0$, i.e.

$$\omega_0 = \omega_c - 2J \cos k_{m_0}^A. \quad (\text{S22})$$

Also, to ensure the weak-coupling regime, we assume that $g \ll J$ and that $\omega_0 \equiv \omega_{m_0}$ is sufficiently far from the band edges $\omega_c \pm 2J$ (where singularities occur). Accordingly, we can effectively approximate the dispersion law of block A to the first order around $m = m_0$ as

$$\omega_m^A \simeq \omega_0 + v(k_m - k_{m_0}) = \omega_0 + v \frac{\pi}{N_A + 1} \nu, \quad (\text{S23})$$

where we used Eq. (S23) and replaced the effective group velocity $v = 2J \sin k_{m_0}$. In the last identity, we introduced the integer number $\nu = m - m_0$ (taking both negative and positive values). For analogous reasons, since the coupling strength between the generic block- A mode and block B is much smaller than the waveguide bandwidth in the thermodynamic limit, i.e. $\xi_m \ll J$ [cf. Eq. (S13)], we linearize the dispersion relation of block B as $\omega^B(k) \simeq \omega_0 + vk$, where k now runs between $-\infty$ and $+\infty$ and approximate ξ_m [cf. Eq. (S13)] to the lowest order around k_{m_0} obtaining

$$\xi_m \simeq J \sqrt{\frac{2}{N_A + 1}} (-1)^m \sin(k_{m_0}) = \frac{v}{2} \sqrt{\frac{2}{N_A + 1}} (-1)^\nu. \quad (\text{S24})$$

Final continuous Hamiltonian

Putting everything together we get the total Hamiltonian

$$\begin{aligned} \hat{H}_F &= \sum_{\nu=-\infty}^{\infty} \Omega_\nu \hat{\alpha}_\nu^\dagger \hat{\alpha}_\nu + \int_0^\pi dk \omega(k) \hat{\beta}^\dagger(k) \hat{\beta}(k) + \sum_{\nu=-\infty}^{\infty} \frac{v}{2} \sqrt{\frac{2}{N_A + 1}} (-1)^\nu \left(\hat{\alpha}_\nu \int_0^\pi dk \sqrt{\frac{2}{\pi}} \hat{\beta}^\dagger(k) + \text{H.c.} \right) \\ \hat{V}_{AF} &= \sum_{\nu=-\infty}^{\infty} g_\nu \hat{\sigma}_+ \hat{\alpha}_\nu + \text{H.c.}, \end{aligned} \quad (\text{S25})$$

where g_ν is just (S11) expressed in terms of $\nu = m - m_0$ and $\phi = 2k_{m_0}n_0$.

$$g_\nu = g \sqrt{\frac{2}{N_A + 1}} \sin \left(\nu \frac{\pi}{N_A + 1} n_0 + \frac{\phi}{2} \right), \quad (\text{S26})$$

with $\Omega_\nu = \omega_0 + vk_\nu$ and $\omega(k) = \omega_0 + vk$. Each mode ν of the cavity is coupled to block- B with strength $\sim v/\sqrt{N_A}$, which for N_A large enough will be far smaller than v . This and the fact that the coupling of each mode to block- B modes is flat (i.e., frequency-independent) yields that the integrals over k can be extended to the entire real axis. By passing in addition to the frequency domain (using $\omega = vk$ and $\hat{\beta}(k) = \hat{\beta}(\omega)/\sqrt{v}$), we get the free-field Hamiltonian in the form

$$\hat{H}_F = \sum_{\nu} \Omega_\nu \hat{\alpha}_\nu^\dagger \hat{\alpha}_\nu + \int_{-\infty}^{\infty} d\omega \omega \hat{\beta}^\dagger(\omega) \hat{\beta}(\omega) + \sum_{\nu} \sqrt{\frac{v}{N_A + 1}} \left(\hat{\alpha}_\nu \int_{-\infty}^{\infty} d\omega \sqrt{\frac{1}{\pi}} \hat{\beta}^\dagger(\omega) + \text{H.c.} \right), \quad (\text{S27})$$

where we also redefined the cavity modes as $\hat{\alpha}_\nu \rightarrow (-1)^\nu \hat{\alpha}_\nu$, in a way that factor $(-1)^\nu$ is now incorporated in the definition of the emitter-cavity. The latest step is to take the continuous limit of the tight binding model, which essentially leads to the replacement $N_A + 1 \rightarrow L_A$, which leads to Eqs. (3)-(5) in the main text.

SPONTANEOUS EMISSION IN THE MARKOVIAN REGIME

It is well-known that Hamiltonian (1) implies that the atom's excitation amplitude $\epsilon(t)$ obeys the exact delay differential equation [S1, S2]

$$\dot{\epsilon}(t) = -\frac{\Gamma}{2} \epsilon(t) + \frac{\Gamma}{2} e^{i\phi} \epsilon(t - \tau) \Theta(t - \tau). \quad (\text{S28})$$

For very short time delay (Markovian regime), we can replace $t - \tau \simeq t$, so that (S28) reduces to

$$\dot{\epsilon} = -\frac{\Gamma}{2}\epsilon + \frac{\Gamma}{2}e^{i\phi}\epsilon = i\frac{\Gamma}{2}\sin\phi\epsilon - \frac{\Gamma}{2}(1 - \cos\phi)\epsilon. \quad (\text{S29})$$

Hence, the excited-state population will decay as $|\epsilon|^2 = e^{-\Gamma't}$ with

$$\Gamma' = \Gamma(1 - \cos\phi) = 2\Gamma\sin^2\frac{\phi}{2}. \quad (\text{S30})$$

One block- A mode

Consider the effective Hamiltonian (3) and approximate it by retaining only the block- A resonant mode $\nu = 0$, which is justified in the limit of very short time delay. Also, we take $L = x_0$, hence [cf. Eq. (5)]

$$g_0 = g\sqrt{\frac{2}{L}}\sin\frac{\phi}{2}. \quad (\text{S31})$$

Let the atom initially in state $|e\rangle$ with mode $\nu = 0$ and all the modes of block B initially in the vacuum state. Then the joint state of the atom and mode $\nu = 0$ has the form

$$|\Psi(t)\rangle = \epsilon(t)|e, 0\rangle + a_0(t)|g, 1\rangle \quad (\text{S32})$$

with $|e, 0\rangle$ ($|g, 1\rangle$) the state where the atom is in the excited (ground) state while mode $\nu = 0$ has zero (one) photon, where $\epsilon(t)$ and $a_0(t)$ fulfill the differential system (we set in a rotating frame such that $\omega_0 = 0$)

$$\dot{\epsilon} = -ig_0\alpha_0 \quad \dot{\alpha}_0 = -\frac{\gamma}{2}\alpha_0 - ig_0\epsilon$$

subject to the initial condition $\epsilon(0) = 1$, $\alpha_0(0) = 0$.

In the Laplace domain (variable t replaced by s), the system reads

$$s\tilde{\epsilon} - 1 = -ig_0\tilde{\alpha}_0 \quad s\tilde{\alpha}_0 = -\frac{\gamma}{2}\tilde{\alpha}_0 - ig_0\tilde{\epsilon}. \quad (\text{S33})$$

In the limit of very short delay, we get $\gamma \gg g_0$ [cf. Eqs. (4)-(5)]; hence we can replace $\alpha(t)$ with its stationary value for given $\epsilon(t)$ which is equivalent to setting $s = 0$ in the second identity of Eq. (S33). This yields $\tilde{\alpha}_0 = -i\frac{2g_0}{\gamma}\tilde{\epsilon}$. Replacing in the equation for $\tilde{\epsilon}$ we get

$$\tilde{\epsilon} = \frac{1}{s + \Gamma'}, \quad (\text{S34})$$

where $\Gamma' = \frac{2g_0^2}{\gamma}$ matches Eq. (S30).

TENSOR NETWORK SIMULATIONS

The exact results throughout the main text are obtained by leveraging the MPS formalism specifically adapted for photonic circuits featuring time delays, as illustrated in [S3]. We consider the reduced quantum state of the emitter A and the non-Markovian bath F (field in the region within the atom and the mirror) as initially uncorrelated, i.e. $\rho_{AF}(t=0) = \rho_A(0) \otimes \rho_F(0)$. For a single emitter coupled to a semi-infinite waveguide, a simplification of the problem's geometry arises by transforming the configuration into an equivalent one with a chiral infinite waveguide and the emitter coupled to the waveguide at two points separated by a distance of $2x_0$ [S4]. In the interaction picture with respect to the bath and the emitter free Hamiltonians, Eq. (1) can be recast as [S5]:

$$\hat{H}(t) = \hat{H}_{\text{dr}} + g(\hat{\sigma}_A^+(\hat{b}_t + e^{i2\omega_0\tau}\hat{b}_{t-2\tau}) + \text{H.c.}) \quad (\text{S35})$$

where we are including a classical driving Hamiltonian on the atom $\hat{H}_{\text{dr}} = \Omega(\sigma_A^+ + \sigma_A^-)$ and \hat{b}_t are the time-domain ladder operator of the chiral bath. The overall state ρ_{AF} is evolved according to a stroboscopic map with discrete

time steps Δt chosen to be small compared to the relevant frequencies of the system, consistent with the approach used in quantum collision models [S6]. Hence we define the discrete-time propagator

$$\hat{U}_n = \exp\left\{-i\hat{H}_n\Delta t\right\}, \quad (\text{S36})$$

with

$$\hat{H}_n = \hat{H}_{\text{dr}} + \frac{g}{\sqrt{\Delta t}}(\hat{\sigma}_A^+(\hat{b}_n + e^{i\phi}\hat{b}_{n-\ell}) + \text{H.c.}), \quad (\text{S37})$$

where we introduced the discrete bosonic noise operators $\hat{b}_n = \frac{1}{\sqrt{\Delta t}} \int_{t_{n-1}}^{t_n} \hat{b}(s)ds$ and $\ell = 2\tau/\Delta t$. The discretization of the interaction reflects in the representation of the environment as a chain of ℓ quantum harmonic oscillators and the joint state of atom and environment as

$$\rho_{AF} = \sum_{\vec{i}, \vec{i}'} c_{\vec{i}, \vec{i}'} |\vec{i}\rangle \langle \vec{i}'| \quad (\text{S38})$$

with the basis state $|\vec{i}\rangle = |i_A, i_1, \dots, i_\ell\rangle$, where the numbers identify the ℓ oscillators. This representation can be reformulated using singular value decomposition between each possible bipartition of the chain, yielding a Matrix Product Operator (MPO)

$$\rho_{AF} = \sum_{\vec{i}, \vec{i}'} \sum_{\vec{\kappa}} A_{\kappa_1}^{i_A, i'_A} A_{\kappa_1, \kappa_2}^{i_1, i'_1} \dots A_{\kappa_{\ell-1}}^{i_{\ell-1}, i'_{\ell-1}} |\vec{i}\rangle \langle \vec{i}'|. \quad (\text{S39})$$

Here, the indices \vec{i} and \vec{i}' iterate over the computational basis of each subsystem (*physical indices*), and the contracted indices $\vec{\kappa}$ (*virtual or bond indices*) run from 0 to a maximum value D_{max} called *bond dimension*, capturing correlations between the sites [S7, S8]. Truncating the bond dimension up to a certain threshold corresponds to discarding the smallest singular values in the decomposition mentioned above. This approximation proves highly effective, especially when the subsystems exhibit weak correlations, significantly reducing the computational resources required to manage the state. Any operator can be expressed as a Matrix Product Operator (MPO) and operates on the state by contracting the relevant physical indices. After the action of a non-local operator, the bond dimension between two sites involved in the evolution typically increases. Therefore, a *compression* step, i.e., truncation of the bond dimension, is always performed to effectively manage the dimension of the tensor network. In particular, the propagator (S36) features terms acting on A and on two oscillators (the 1st and the ℓ th) at the same time. Given the high cost of compression for long-range interactions, we mitigate this by simplifying the propagator to the application of nearest neighbor unitary operations. This is achieved through a suitable swap scheme that maintains the physics unaltered [S3, S9]. The complete process of evolution-update is illustrated in Fig. S2 a-d, utilizing the Penrose notation for tensors. This scheme can be directly applied to spontaneous-emission dynamics without modification. For scattering dynamics, an additional step is necessary to represent the incident pulse because the incoming field constitutes a correlated state across multiple oscillators. Let m be the number of such oscillators. Thus we define the discrete n -particle wavepacket operator as

$$\hat{\psi}_n^\dagger = \left(\sum_{i=0}^m \sqrt{\Delta t} \xi_i \hat{a}_i^\dagger\right)^n, \quad (\text{S40})$$

where ξ_i is a discrete sample of the Gaussian amplitude

$$\xi(t)_{t_0} = \left(\frac{W^2}{2\pi}\right)^{1/4} \exp\left\{\frac{1}{4}W^2(t-t_0)^2\right\}, \quad (\text{S41})$$

with W and t_0 the frequency bandwidth and the center of the pulse respectively. The coherent-state pulse with average photon number $|\alpha|^2$ reads [S11]

$$|\psi\rangle_{\text{pulse}} = e^{-|\alpha|^2/2} \sum_{n=0}^{\infty} \frac{\alpha^n}{n!} \hat{\psi}_n^\dagger |0\rangle. \quad (\text{S42})$$

This state can be generated as a Matrix Product Operator (MPO) by applying the tensor network corresponding to (S40) to a chain of m oscillators initially in the vacuum state. For low powers, the first terms of the sum above

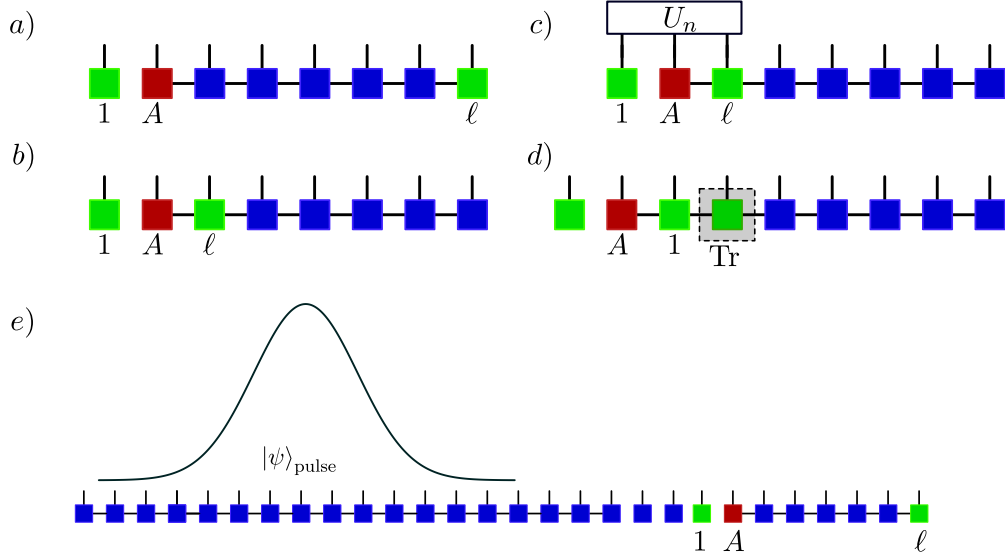


FIG. S2. Update of the MPO representing the joint state of the atom and the non-Markovian bath according to (S39). The tensor in red represents A^{i_A, i'_A} , indicating the atom's state. The blue tensors correspond to the chain's harmonic oscillators, while the green ones represent the first and ℓ th oscillators of the chain, which interact with the atom. Each physical leg denotes the pair of vector spaces corresponding to each tensor. Consequently, the operators acting on the chain should be understood as the corresponding maps, or equivalently, the operators acting on the local purification form matrix product state (PMPS) of the system's density matrix [S10]. a) After the $n - 1$ th step the joint atom-bath system and the oscillator 1 on the left are uncorrelated. b) The ℓ th oscillator is put on the right of the atom through a sequence of swap operations (not depicted). c) the tensor network corresponding to the propagator (S36) acts on the systems 1, A and ℓ . d) After the interaction, the ℓ th oscillator is traced, A and 1 swap their positions, and a new uncorrelated oscillator is added to the left. A compression follows after each transformation of the chain. e) Initial state for the scattering dynamics. A chain of oscillators encoding the state of the incoming pulse is placed on the left of the joint atom-bath system.

are sufficient to represent the pulse. The atomic population, ε , the output field intensity I_{out} , and the two-photon correlation function, $G^{(2)}$, are obtained through measurements on the reduced state of the atom, $\hat{\rho}_A(t) = \text{Tr}_F\{\hat{\rho}_{AF}(t)\}$, and of the ℓ th oscillator, $\hat{\rho}_\ell(t) = \text{Tr}_{AF \setminus \ell}\{\hat{\rho}_{AF}(t)\}$ respectively:

$$\varepsilon(t) = \text{Tr}\{\hat{\rho}_A(t)\hat{\sigma}_+\hat{\sigma}_-\}, \quad (\text{S43})$$

$$I_{\text{out}}(t) = \text{Tr}\{\hat{\rho}_\ell(t)\hat{a}_\ell^\dagger(t)\hat{a}_\ell(t)\}, \quad (\text{S44})$$

$$G^{(2)}(t) = \text{Tr}\{\hat{\rho}_\ell(t)\hat{a}_\ell^\dagger(t)\hat{a}_\ell^\dagger(t)\hat{a}_\ell(t)\hat{a}_\ell(t)\}. \quad (\text{S45})$$

INPUT OUTPUT FORMALISM FOR THE EFFECTIVE MODEL

To simulate the scattering of a photonic wavepacket with the emitter within our effective model we treat the block B waveguide modes, $\hat{\beta}_\omega$, as a Markovian bath. In this way is possible to eliminate these degrees of freedom obtaining the following master equation for an open multimode cavity QED system

$$\dot{\hat{\rho}} = -i[H_{\text{CQED}} + H_D, \hat{\rho}] + \sqrt{\gamma}\mathcal{D}[\hat{A}]\hat{\rho}, \quad (\text{S46})$$

where

$$H_{\text{CQED}} = \omega_0 \hat{\sigma}_+\hat{\sigma}_- + \sum_\nu \Omega_\nu \hat{\alpha}_\nu^\dagger \hat{\alpha}_\nu + \sum_\nu g_\nu (\hat{\alpha}_\nu^\dagger \hat{\sigma}_- + \text{H.c.}) \quad (\text{S47})$$

is the system Hamiltonian with Ω_ν and g_ν being defined in the main text. In Eq. (S46) we introduced the usual Lindbladian dissipator $\mathcal{D}[\hat{A}]\rho = \hat{A}\rho\hat{A}^\dagger - \{\hat{A}^\dagger\hat{A}, \rho\}/2$ applied to the collective mode operator $\hat{A} = \sum_\nu \hat{\alpha}_\nu$ with $\gamma = 2v/L$ being the decay rate of block A into the block B bath. In Eq. (S46) we included a coherent driving term of the modes

α_ν :

$$H_D = \sqrt{\gamma} \sum_{\nu} [E_{\text{in}}(t) e^{i\omega_{\text{in}} t} \hat{\alpha}_{\nu}^{\dagger} + \text{H.c.}] \quad (\text{S48})$$

where ω_{in} is the frequency of the driving input field. The shape of the input pulse is determined by the field amplitude $E_{\text{in}}(t)$, normalized with respect to the number of photons n_{ph} , $\int dt |E_{\text{in}}(t)|^2 = n_{\text{ph}}$. For the scattering process discussed in the main text, we employ the same Gaussian pulse shape as specified in Eq. (S41), $E_{\text{in}}(t) := \xi(t)_{t_0}$. The open-system dynamics of the multimode cavity QED system, described by Eq. (S46), is simulated using a quantum trajectories approach, averaging over $n_t = 4000$ trajectories [S12]. Once solved the system dynamics the output field can be reconstructed using the following input-output equation [S13]:

$$\hat{E}_{\text{out}}(t) = \hat{E}_{\text{in}}(t) + i\sqrt{\gamma} \sum_{\nu} \hat{\alpha}_{\nu}(t). \quad (\text{S49})$$

The intensity of the output field and the two-photon correlation function can then be computed in terms of the modes of the effective cavity and read $I_{\text{out}}(t) = \langle \hat{\alpha}_{\nu}^{\dagger}(t) \hat{\alpha}_{\nu}(t) \rangle$ and $G^{(2)}(t) = \langle \hat{\alpha}_{\nu}^{\dagger}(t) \hat{\alpha}_{\nu}^{\dagger}(t) \hat{\alpha}_{\nu}(t) \hat{\alpha}_{\nu}(t) \rangle$, respectively.

-
- [S1] U. Dorner and P. Zoller, *Physical Review A* **66**, 1 (2002).
[S2] T. Tufarelli, F. Ciccarello, and M. S. Kim, *Physical Review A* **87**, 13820 (2013).
[S3] H. Pichler and P. Zoller, *Phys. Rev. Lett.* **116**, 093601 (2016).
[S4] Y. L. L. Fang, F. Ciccarello, and H. U. Baranger, *New Journal of Physics* **20**, 43035 (2018).
[S5] D. Cilluffo, A. Carollo, S. Lorenzo, J. A. Gross, G. M. Palma, and F. Ciccarello, *Phys. Rev. Research* **2**, 043070 (2020).
[S6] F. Ciccarello, S. Lorenzo, V. Giovannetti, and G. M. Palma, *Physics Reports* **954**, 1–70 (2022).
[S7] U. Schollwöck, *Annals of Physics* **326**, 96 (2011), arXiv:1008.3477.
[S8] G. Vidal, *Physical Review Letters* **91**, 147902 (2003), arXiv:0301063 [quant-ph].
[S9] J. Schachenmayer, I. Lesanovsky, A. Micheli, and A. J. Daley, *New Journal of Physics* **12**, 103044 (2010).
[S10] G. D. I. Cuevas, N. Schuch, D. Pérez-García, and J. Ignacio Cirac, *New Journal of Physics* **15**, 123021 (2013).
[S11] H. Zheng, D. J. Gauthier, and H. U. Baranger, *Physical Review A* **82** (2010), 10.1103/PhysRevA.82.063816, arXiv:1009.5325.
[S12] K. Mølmer, Y. Castin, and J. Dalibard, *J. Opt. Soc. Am. B* **10**, 524 (1993).
[S13] C. W. Gardiner and M. J. Collett, *Phys. Rev. A* **31**, 3761 (1985).